

## Lasers in Manufacturing Conference 2025

# Laser-Based Drying of PEMFC Catalyst Layers

Manuella Guirgues<sup>a</sup>, Samuel Fink<sup>a</sup>, Sathishkumar Natarajan<sup>a</sup>

<sup>a</sup>*Fraunhofer Institute for Laser Technology ILT, Steinbachstraße 15, Aachen 52074, Aachen*

### Abstract

With the production speed being a major obstacle in the economic production of polymer exchange membrane fuel cells (PEMFCs), introducing laser based drying of the coated catalyst layers could bring drying times from minutes down to just a few seconds. Laser-based drying is also a more efficient alternative to oven drying and has a much smaller footprint. In this paper we present the effects of the laser irradiation on the catalyst layer, demonstrating the degree of drying and the microstructure of the laser-based dried catalyst layers at different drying temperatures and interaction times. For this purpose, a 980nm diode laser with a closed temperature control loop is used to dry screen printed catalyst layers in a semi-continuous process.

Keywords: PEMFC production; Laser-based drying; Membrane Electrode Assembly (MEA) production

### 1. Introduction

Over the course of the last decade, the demand for polymer electrolyte membrane fuel cells (PEMFCs) has risen steadily since they have a high-power density, the ability to operate at low temperatures and create no emissions (Kumar, et al. 2025). At the heart of PEMFC is the polymer electrolyte membrane with the electrodes on either side, followed by the subgasket material which offers a gastight seal for this Membrane electrode assembly (MEA) and provides some mechanical strength to enable easier handling of the membranes for stacking. Another component is the gas diffusion layer and finally the bipolar plates. These single cells are stacked and finally sandwiched between a current collector plate and an endplate (Kumar, et al. 2025). The electrodes are usually made of large porous carbon particles which act as a scaffold for platinum nanoparticles along with an ionomer that acts as a binder as well as a transport facilitator for the protons ensuring efficient electrochemical performance. In order to ensure that the electrode components are homogeneously mixed, these components are dispersed in a solvent or a mixture of solvents, forming an ink/paste that is first coated on a substrate and then dried using convection ovens (Orfanidi, et al. 2018). Ideally, the substrate would be the PEM, this application method of the electrodes is known as direct coating, however, it is not commonly used in the roll-to-roll production of MEAs. This is because the solvents in the electrode cause swelling of the membrane. Slower drying allows the solvent more time to penetrate into the membrane, increasing the swelling (Yi und Bae 2017). Meanwhile, speeding up the drying process by increasing the drying temperature is an option limited by the glass transition temperature of the PEM, which when exceeded can cause its degradation and reduce the performance of the fuel cell. To avoid the challenges associated with direct coating, a decal foil material which is not as temperature sensitive and onto which the electrodes adhere less strongly than the PEM is usually used. The electrode ink is coated on this decal foil, dried and transferred onto the PEM via heat pressing. While this process is more popular, its disadvantages are the extra process step, and the decal foil is mostly discarded as a manufacturing waste product.

#### 1.1. Laser-based drying

In comparison to conventional thin film drying methods, laser-based drying offers three main advantages. Firstly, the heat is generated directly in the electrode layer due to absorption of the laser radiation, making the energy deposition more efficient. Secondly, lasers can emit high energy densities which speed up the drying process, reducing the drying module

footprint and the membrane swelling in the direct coating method. Finally, lasers can be controlled very quickly and precisely, ensuring that the desired temperatures can be achieved within a few seconds while preventing the electrode layer from overheating.

## 2. Setup and Process

For the laser drying an LDM2000 compact diode laser with a maximum laser power output of 2kW and an OTX-5 optic from Laserline GmbH are used. The laser radiation wavelength is 980 nm and through mounting the optic on a movable Y-axis a spot size of  $300 \times 300 \text{ mm}^2$  is achieved at a working distance of 600mm. To enable mass transfer, a flow of nitrogen gas is built in with an exhaust system across from it to ensure efficient solvent vapor removal. To measure the surface temperature of the electrode layer, a precision IR camera PI 450i from Optis GmbH & Co.KG is used. For temperature controlled drying this camera is connected to PID controller which controls the laser input signal based on the temperature of the hottest pixel on the electrode surface recorded by the IR camera. The set-up within the housing is depicted in Fig.1.

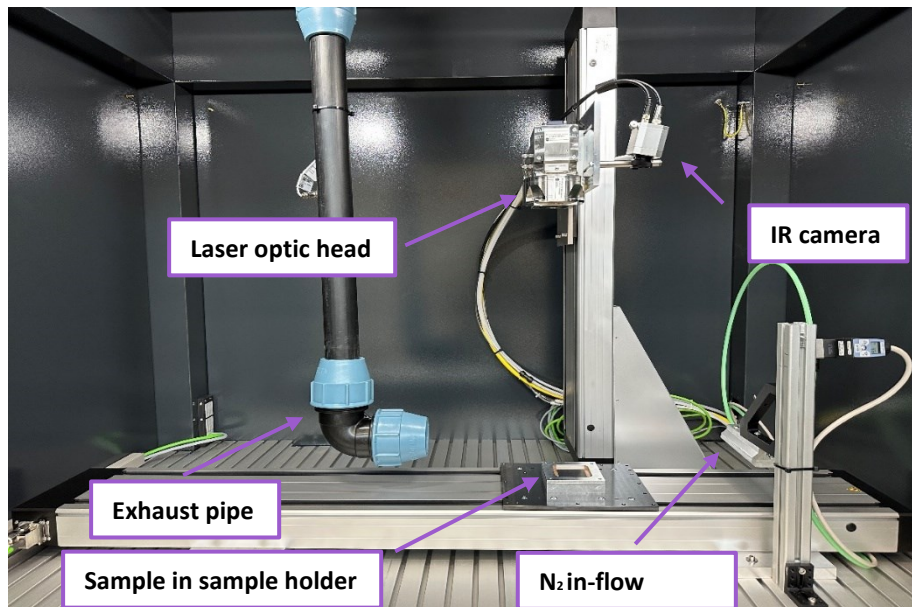


Fig.1. Experimental setup for laser-based drying of PEMFC electrodes

The cathode paste which is described in Table 1 is developed by the Fraunhofer ISE for screen printing and is printed as  $50 \times 50 \text{ mm}^2$  active areas onto a PTFE coated glass fiber fabric of thickness 145  $\mu\text{m}$ , which serves as a decal foil using the RP3.0 half-automated screen printing machine from RokuPrint GmbH. The substrates with the wet cathode layer are then placed onto a aluminum frame which clamps the uncoated edges of the deal foil. This way the coated area is floating. This is done to reduce thermal energy dissipation from the sample onto any metallic horizontal surface beneath it and to ensure a more homogenous temperature profile along the cathode surface. The sample holder containing the sample is then placed underneath the laser optic head to be dried.

Table 1. Chemical composition of the cathode paste (Ney, et al. 2025)

Component	Mass (%)
Elyst Pt50 0550 (Umicore AG & Co. KG)	12.39
Aquivion	4.61
Ethylene glycol	19.15
1,2-Propanediol	63.85

### 3. Results

#### 3.1. Preliminary Experiments

An important parameter to characterize the laser drying process are the optical properties of the substrate and the wet cathode film. To obtain these values the substrate is placed into a LAMDA 1050 UV-VIS-NIR Spectrometer from PerkinElmer, where reflectance  $R$  and transmittance  $T$  are measured. For measuring the optical properties of the wet cathode, a 80  $\mu\text{m}$  thick film is placed between two glass microscope slides which is then placed within the UV-VIS-NIR Spectrometer. The absorption  $A$  is then calculated as:

$$A = 100\% - T - R \quad (1)$$

The Absorption of the wet cathode ink as well as the uncoated PTFE substrate are depicted in Fig.2.(a). The wet cathode ink exhibits an absorption of 95% at the laser's wavelength 980 nm, while the substrate only has an absorption of 16%. Low absorption of laser radiation results in low temperature increases due to laser irradiation. Fig.2.(b) shows a thermographic image of a sample during laser drying. The whole area depicted is irradiated homogeneously with the laser radiation. After 5 s of laser irradiation, the catalyst layer reaches 120°C, meanwhile the irradiated PTFE coated glass fiber decal substrate deviates from room temperature by a few degrees Celsius. Due to the differences in the optical properties, a stable drying process can be achieved without overheating the PTFE foil.

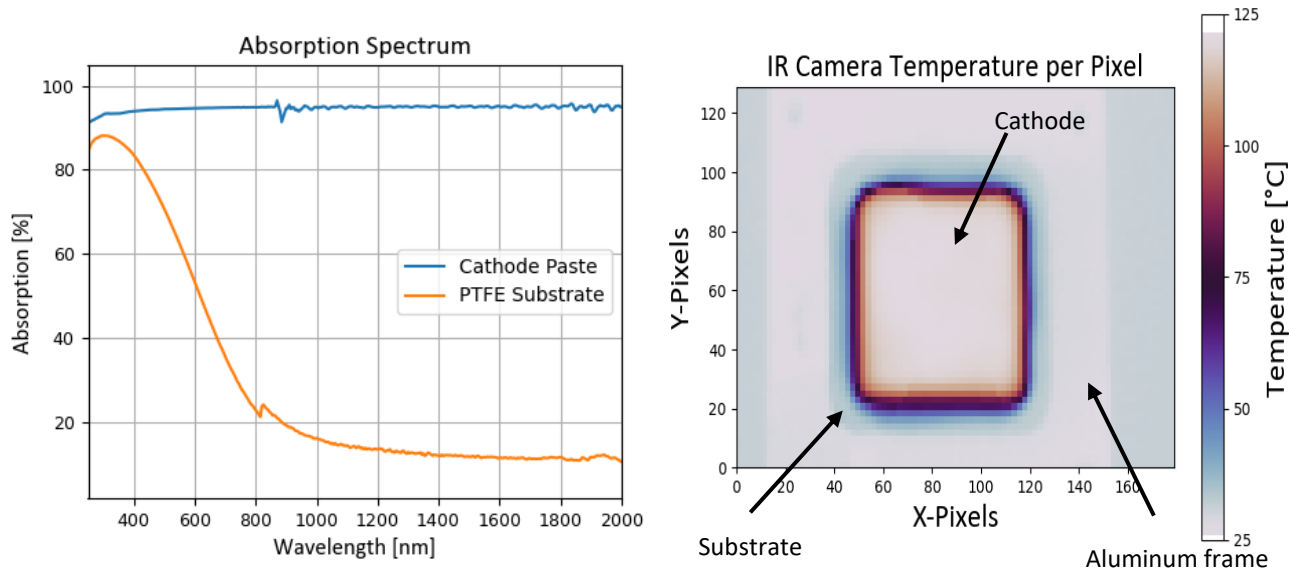


Fig.2. (a) Absorption spectrum of 145  $\mu\text{m}$  PTFE substrate and 80  $\mu\text{m}$  cathode paste (left); (b) Pixelated temperature distribution of a coated sample in the sample holder after 5s of laser irradiation with 120 °C temperature setpoint (right).

#### 3.2. Solvent Content During Drying

To measure the amount of solvent removed from a wet sample, each substrate is weighed three times. Once before coating, then right after coating and after being dried using the above-mentioned set up for a specific period, called the laser interaction time. Using these weight measurements, the mass of the total solvent content per coated layer is determined by knowing the fraction of solvent mass in the cathode paste. According to empirical data (Avci, Can und Etemoglu 2001) of drying of thin films, the drying process occurs over two periods (see Fig. 3.(a)). The first is the constant drying rate period, during which up to 80% of the film's solvent can be removed and the second is the falling drying rate period which

encompasses a sizable proportion of the total drying time. During the falling drying rate period the drying rate becomes limited by the ability of solvent particles to pass through the solid into the free surface. Figure 3(b) shows that laser-based drying experiments follow a similar solvent content over time profiles as their convection oven counterparts. With a constant laser intensity of  $3 \text{ W/cm}^2$ , 4 s of laser irradiation are required to remove 85.2% of the solvent and another 4 s are required to remove another further 12.8% of the solvent content in a layer with dry thickness of  $5 \mu\text{m}$ .

$$\text{solvent content [%]} = \frac{\text{Mass of solvent in laser dried layer}}{\text{Mass of total solvent in wet layer}} \cdot 100\% \quad (2)$$

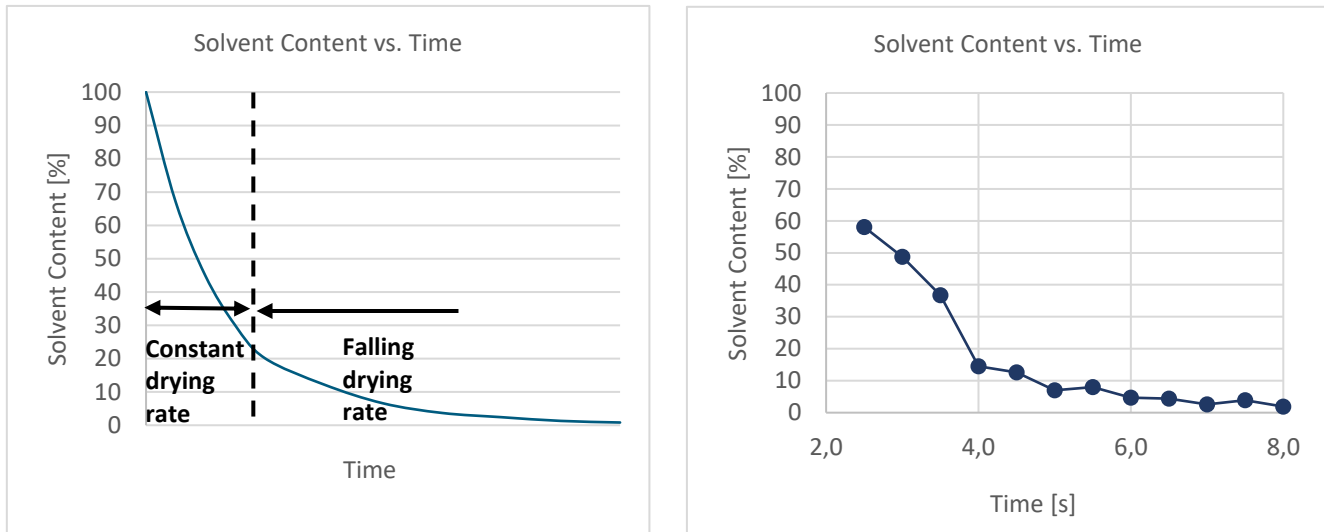


Fig.3. (a) Empirical data: solvent content (Avci, Can und Etemoḡlu 2001) (left); (b) Measured solvent content at a constant laser intensity of  $3 \text{ W/cm}^2$  and a dry layer thickness of  $\sim 5 \mu\text{m}$  (right).

### 3.3. Temperature-Time Profile

According to empirical thin film drying data (Avci, Can und Etemoḡlu 2001), temperature-time profiles also show characteristic features that enable the distinction between the constant drying rate period and the falling drying rate period. Fig 4.(a) depicts the profile of the surface temperature of a thin film during the drying process based on empirical data. During the constant drying period, the temperature remains constant, whereas, during the falling drying rate period the incoming thermal energy both increases the temperature of the film and evaporates the remaining moisture. When comparing Fig 4.(a) with Fig 4.(b), which shows the measured surface temperature profile of a cathode layer being irradiated at a constant laser intensity of  $0.22 \text{ W/cm}^2$  and has a dry layer thickness of  $\sim 5 \mu\text{m}$ , the constant drying rate and the falling drying rate periods can be deducted as 14.1 s and 15.7 s respectively.

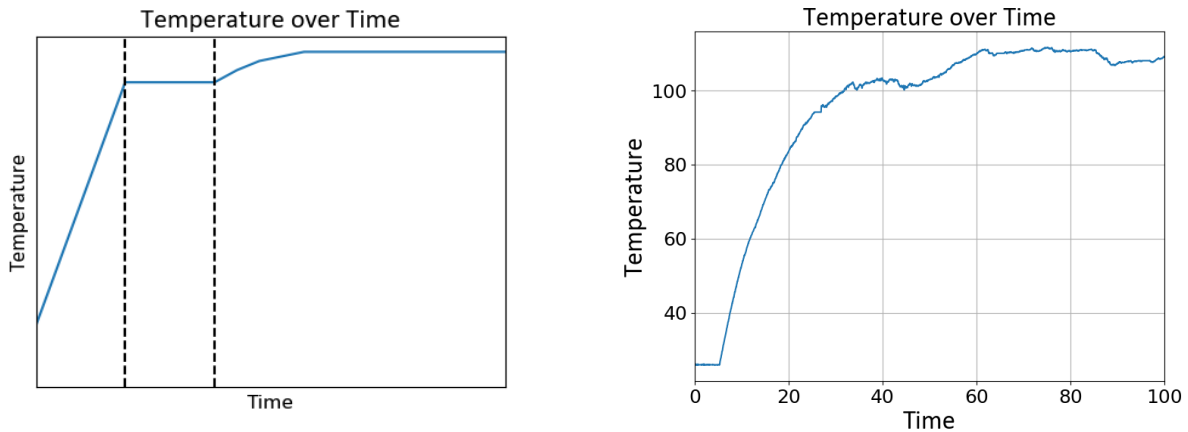


Fig.4. (a) Empirical data: temperature profile during the drying process (Avci, Can und Etemoglu 2001)(left); (b) Measured surface temperature profile at a constant laser intensity of  $0.22 \text{ W/cm}^2$  and a dry layer thickness of  $\sim 5 \mu\text{m}$ (right).

### 3.4. Laser-Based Drying Effects on Crack Formation

Cracks on the drying surface can form due to the shrinkage of the film during drying. These cracks increase the electrical resistance of the fuel cell and can grow over time, further degrading the electrode (Liu, et al. 2024). A solution proven successful in avoiding crack formation during the drying of PEMFC electrodes using convection ovens is the incorporation of a high boiling point solvent e.g., ethylene glycol (see table 1) in the electrode paste (Hasegawa, et al. 2021). To assess if the incorporation of a high boiling point is a viable solution for laser-based drying, the chemical composition of the cathode paste from table 1, the substrate material, the drying time and the paste application process are kept constant, while the drying temperature is varied to ensure different drying speeds. The inspected samples are all subjected to laser irradiated for 120 s to eliminate any residual moisture, after which they are imaged using Scanning Electron Microscopy (SEM) at a magnification of 400x. Figures 5.(a)-(c) show that increasing the drying temperature and hence drying speed did not increase the crack formation in the electrode layers.

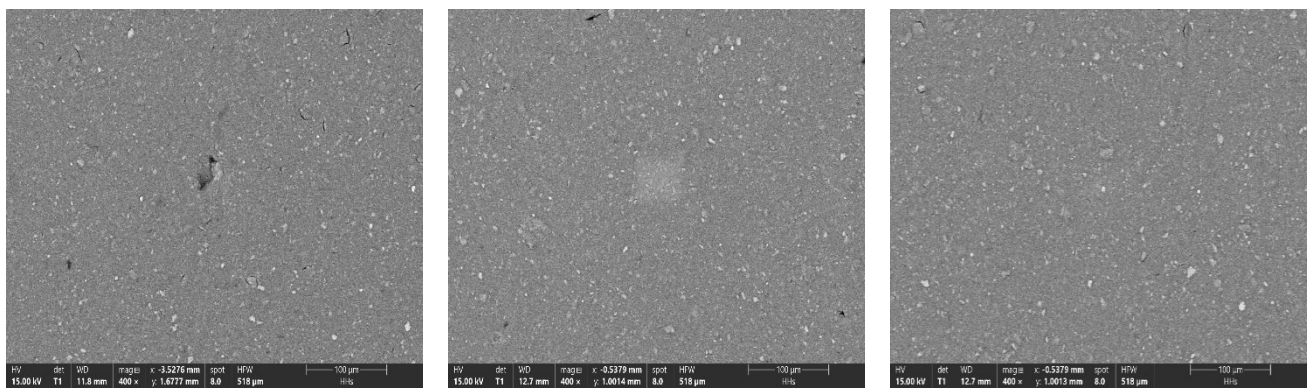


Fig.5. (a) SEM image of sample dried at  $100 \text{ }^\circ\text{C}$  (left); (b) SEM image of sample dried at  $120 \text{ }^\circ\text{C}$  (center) (The bright square observed in the center of the figure is a measurement artifact resulting from the interaction of the electron beam SEM with the cathode.); (c) SEM image of sample dried at  $140 \text{ }^\circ\text{C}$  (right)

Finally, a sample dried in a convection oven at  $120 \text{ }^\circ\text{C}$  for 300 s to ensure complete moisture removal is also inspected with SEM imaging at a magnification of 400x and compared with a laser dried sample at  $120^\circ\text{C}$  for 2 mins. Figures 6(a) and 6(b) demonstrate that laser-based drying does not increase the crack formation when compared to oven dried samples subjected to similar drying conditions.

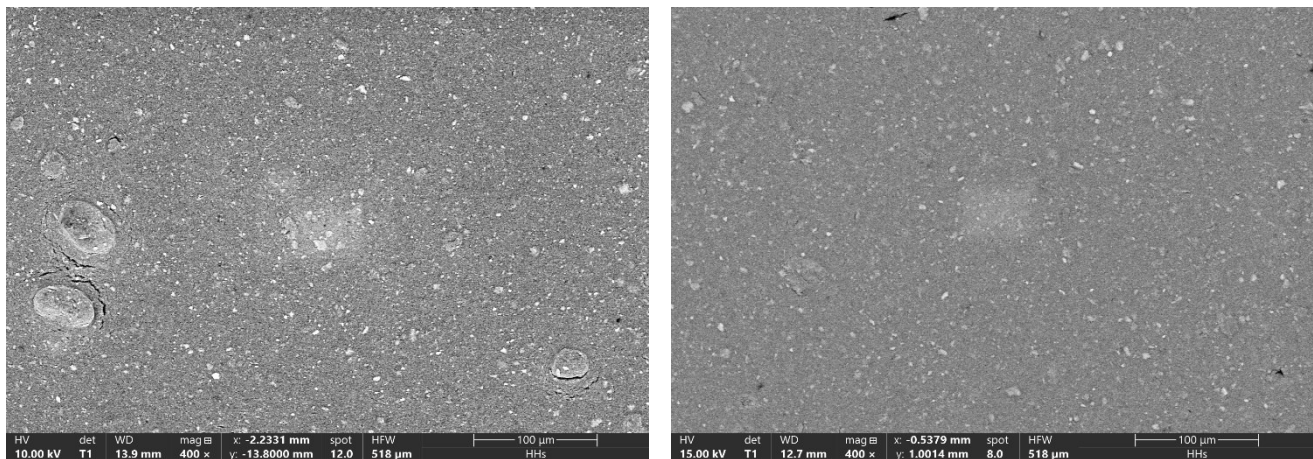


Fig.6. (a) SEM image of an oven dried sample for 5 mins at 120°C air temperature. The protruding particles depicted in this figure are agglomerates that likely result from extended storage periods of the paste prior to application, around which cracks develop during drying. This issue can be mitigated by increasing the stirring time of the paste before application; (b) SEM image of a laser dried sample for 2 mins at 120°C surface temperature. (The bright square observed in the center of the Fig.6.(a) & Fig.6.(b) is a measurement artifact resulting from the interaction of the electron beam SEM with the cathode.)

#### 4. Conclusion

In conclusion, the degree of absorption of laser radiation by both the substrate and the cathode affects the temperatures attained at identical laser intensities. The substrate's temperature increases only a few degrees Celsius above room temperature, attributable to its absorption of 16%. In contrast, the cathode, with an absorption of 95%, reaches a temperature of 120 °C. Additionally, laser radiation with an intensity of 3 W/cm<sup>2</sup> achieves a degree of drying of 98% within 8 seconds for a dry cathode thickness of 5 μm. Furthermore, scanning electron microscopy (SEM) imaging indicates that increasing the laser-induced drying temperature does not lead to visible crack formation within the cathode during the drying process. Finally, SEM imaging of laser and oven dried electrodes demonstrates that laser radiation does not induce crack formation in the cathode layer when dried under conditions similar to those in a convection oven. These investigations represent initial steps toward laser-based drying, possibly enabling the direct coating of temperature-sensitive PEM materials, provided their absorption of the laser wavelength used in the drying process is lower than that of the electrode paste. Furthermore, the reduced drying times associated with laser-based drying could be leveraged in the future within a roll-to-roll production process of MEAs at web speeds exceeding 10 m/min.

#### Acknowledgements

We would like to express our gratitude towards the hydrogen fuel cell production team at the Fraunhofer ISE (Freiburg, Germany) for providing us with the cathode paste used in all experiments presented in this paper.

#### References

Avcı, Atakan, Muhiddin Can, and Akin B Etemoğlu. 2001. "A theoretical approach to the drying process of thin film layers." *Applied Thermal Engineering, Volume 21, Issue4* 465-479.

Hasegawa, Naoki, Atsushi Kamiya, Takuro Matsunaga, Naoki Kitano, and Masashi Harada. 2021. "Analysis of crack formation during fuel cell catalyst ink drying process. Reduction of catalyst layer cracking by addition of high boiling point solvent." *Colloids and Surfaces A: Physicochemical and Engineering Aspects, Volume 628*.

Kumar, Vijay Bhooshan, Aakash Collin, M.Gop Sankar, and Kanakasabapathi Subramanian. 2025. "Fuel cell technologies in the automotive sector: A focus on proton exchange membrane and Alkaline fuel cells." *Green Technologies and Sustainability*.

Liu, Pengcheng, Daijun Yang, Bing L, Jialun Kang, Cunman Zhang, Pingwen Ming, Xiangmin Pan, and Hengzhi Liu. 2024. "Benzoic acid as additive: A route to inhibit the formation of cracks in catalyst layer of proton exchange membrane fuel cells." *Journal of Power Sources, Volume 591*.

Ney, L., N. Seidl, R. Singh, P. Schneider, D. Stross, A. Göppentin, S. Tepner, and M. and Keding, R. Klingele. 2025. "Screen Printing Catalyst Inks With Enhanced Process Stability for PEM Fuel Cell Production." *Fuel Cells*, 25: e202400158.

Orfanidi, Alin, Philipp J. Rheinländer, Nicole Schulte, and Hubert A. Gasteiger. 2018. "Ink Solvent Dependence of the Ionomer Distribution in the Catalyst Layer of a PEMFC." *Journal of The Electrochemical Society*.

Yi, Young Don, and Young Chan Bae. 2017. "Swelling behaviors of proton exchange membranes in alcohols." *Polymer Volume 130* 112-123.